2.25 CONVECTIVE STORM INITIATION IN WESTERN CATALONIA: CHARACTERISTICS AND UNCERTAINTIES OF THE METHODOLOGY USED

Ramon Pascual
Instituto Nacional de Meteorología,
Barcelona, Spain

1. INTRODUCTION

Forecasting of convection initiation is one of the main current challenges in operational nowcasting tasks in the Spanish National Weather Service. Knowledge of areas where convection develops most frequently is a previous step to obtain accurate nowcasts.

Pascual *et al.* 2004 determined location and timing of storm initiation over central Catalonia during June, July, August and September 2003 by examining radar reflectivity data at 10 min intervals. For each day, regions of convective initiation were identified using two methods: one indirect determining diurnal relative frequencies of radar reflectivity and another direct identifying and tracking the potentially convective cells with and operational automated algorithm.

The second method described above was used to analyze the convection initiation for 27 hailstorms occurred over western Catalonia between April and October, from 2000 to 2003. In this study, however, a further careful subjective analysis have been made to discriminate the radar-detected storm initiation locations associated to meteorological phenomena from those linked to effects related with the observational method itself and the specific characteristics of the algorithms used. Uncertainties in radar measurements must be taken into account before to establish conclusions about convection characteristics (Howard *et al.* 1997).

A set of different artifacts has appeared when examining the 27 radar image loops: false splitting, old cells rebirth, ground clutter echoes intensification (anaprop) and alternation in characterization of a storm as a single cell or a multicell storm. These artifacts could be considered as part of a general problem of tracking complex visual objects from the point of view of radar.

* *Corresponding author address:* Ramón Pascual, Instituto Nacional de Meteorología, Arquitecte Sert 1, Barcelona, 08005, Spain; e-mail: ramonp.bar@inm.es

"Visual" phenomena such as agile motion, distractions, and occlusions (Rasmussen and Hager 2001) interfere with identification and tracking of radar structures. It is therefore necessary to extract these artifacts from the total set of storm initiation locations before to characterize storm initiation in this area.

The use of radar data to analyze convection initiation has suggested to associate development of new convective cells to the presence of a planetary boundary layer convergence zone (Wilson and Schreiber 1986; Koch and Ray 1997). Previous studies carried out in Catalonia (Pascual and Callado 2002) have analyzed subjectively the origin of convection identified in radar data with low levels convergence features. The last part of this paper presents a similar analysis and tries to show the link with the population of automated new convective cells identified.

2. STUDY AREA

Catalonia is located at the northeastern Spain corner and is limited by the Mediterranean Sea (by the East and South), the Pyrenees range at the North, and the Ebro river valley at the West. The Pyrenees and the two ranges extending from northeast to southwest and located parallel to the coast are the more relevant topographic elements. To the west of these coastal ranges flat terrain, surrounded by the Pyrenees in the north side and the Iberian Mountains in the south side, extends over more than 300 km all along the Ebro river valley.

The study area is a rectangle defined by the geographical coordinates: 41.3ºN and 41.9ºN ; 1.3ºE and 0.3ºW, and located in western Catalonia plains and its westward prolongation. The dimensions of the rectangle are 130 km long, 70 km wide and 9100 km^2.

3. DATA AND METHODOLOGY

Main characteristics of the Doppler radar used in this study are given in section 3.1. The other tools used and their role in the identification and characterization of convective structures are given in section 3.2.

3.1 Doppler radar

The Spanish National Weather Service (INM) has a network of 15 C-band Doppler radars covering almost all the Iberian Peninsula and surrounding maritime areas. The radar of the INM installed in Catalonia is located about 20 km South-West from Barcelona city, and at 654 m above mean sea level (MSL). Table 1 summarizes the principal characteristics of this radar.

Wavelength (cm)	5.4 (C-band)
Resolution (km^2)	2x2
Range (km)	Normal:240
Exploration Interval (min.)	10
Peak Power (kW)	250
Beamwidth (deg.)	0.9º
Pulselenght (m)	Normal: 600

Table 1. Main characteristics of INM Doppler radar used in this study.

From the point of view of the analysis carried out here, it is important to take into account some aspects:

- Lowest elevation scan is 0.5º. As the defined rectangular area is located between 50 km and 180 km from radar, the height of the radar beam centre over this area is comprised between 1.5 km and 5 km.

- Orographic beam blockage is important in a narrow band located in the central zone of the rectangular area. The rest of the area is relatively well observed by radar (Fig. 1).

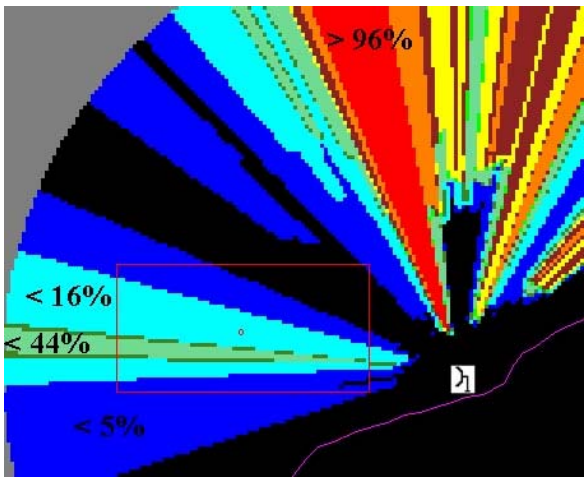

Fig. 1. Orographic beam blockage of the INM-Catalonia radar first elevation. Occultation is in %. The rectangle defines the study area. Here and in the rest of images henceforth North is in the top of the image.

- Studied area is almost free of ground clutter echoes (Fig. 2), as corresponds to a flat area at a low altitude above sea level. There are only significant echoes in the southeastern corner of the area.

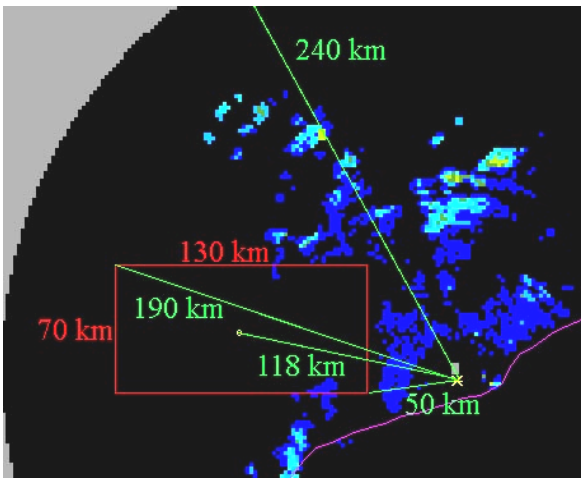

Fig. 2. Mean ground clutter map at the first elevation of the INM radar in Catalonia. Darker blue corresponds to ground clutter from 0 km to 2.5 km. Rectangle dimensions in red and other relevant distances in green. The rectangle defines the study area.

3.2 Complementary data

Hailstorm data from a semiautomatic network belonging to the *Agrupacio de Defensa Vegetal de les Terres de Ponent (*ADV) have been used to select the convective episodes. This network, located in the plains of western Catalonia, covers an area of 3400 km^2 and is inside the rectangle defined above.

Satellite imagery from Meteosat 7 and NOAA-14, 15,16,17 have been used to characterize convective structures (channels VIS and IR), corroborate the presence of convective cells (VIS) and support the synoptic and mesoscale diagnostic (WV).

Numerical model outputs from the INM-HIRLAM Model (0.5 º horizontal resolution) and sea level pressure/frontal analysis charts from the Met. Office have been used to describe synoptic and mesoscale environment and propose origins to the boundary layer convergence zones established from radar imagery.

Finally, Zaragoza INM sounding data (130 km westward the center of the studied area) has been used to estimate instability. The relatively topographical evenness between both areas justifies the use of this information, especially when analyzing stability conditions and middle and high levels flow.

3.3 Radar database

A total of 27 days have been selected from the 43 hailstorms database. An initial database of 3888 polar volumes of radar reflectivity (ZNP) is theoretically available and 751 of those contain relevant information. These have been corrected for ground clutter, orography screening effects, electronic fluctuations, and the general signal decay due to rain over the radome (Sempere-Torres *et al*. 2003). These corrections are fundamental because automated detection of potentially convective radar structures is very sensitive to reflectivity horizontal gradients and local reflectivity values.

Path attenuation by rain and some ground clutter echoes associated to anomalous propagation conditions remain in corrected reflectivity fields introducing several uncertainties in the automated detection and tracking.

3.4 Convective cells origin identification

Identification, tracking and extrapolation software (YRADAR) based on the identification algorithm developed by Steiner *et al.* (1995), is operational on the INM-McIdas system (Martín 2001).

This object-oriented nowcasting tool has been ran over the selected first PPI (PPI0) in Cartesian coordinates generating a set of files that contain information about geographical coordinates, time, dimension, and maximum and mean reflectivity for all the 2D potentially convective structures identified. Henceforth we will name these 2D structures convective cells or cells and will be designated as CEL0, although any 3D analysis has been carried out (In fact a 3D convective cell operational analysis has been also developed in INM (Carretero 2001)). Tracking allowed defining a cell as new when it is not linked to any previous structure (Wilson *et al.* 1986).

The main characteristics of the identification and tracking processes must be taken into account. YRADAR has been developed to identify, characterize, track and extrapolate the more significant convective cells or mature cells present at time *t* in the radar domain. Therefore, it would not expect that YRADAR identify the first echo associated to a cell. However, further subjective analysis carried out has shown that the error in considering 2D new structures centroid coordinates and time to analyze convection initiation is sufficiently small (a maximum delay of 30 ‘) to accept the results presented here as a good first approximation. This is especially true when analyzing the number of convective cells developed and the main triggering mechanisms.

YRADAR considers that a pixel is convective if: Z ≥ 45 dBZ or Z ≥ 40 dBZ and is a local maximum (horizontal gradient criterion) or the pixel is close enough to a convective pixel (neighborhood criterion). YRADAR considers 4-connectivity to build 2D convective cells. Any restriction has been applied to convective cell dimension although for tracking purposes they have been classified as small (< 24 km^2) and large (≥ 24 km^2). Tracking method assigns large cells at instant *t* to the nearest large cells at instant *t-10’*. Small cells have been ever considered as new cells (Martín 2001).

New cells locations have been distributed over an orographic basis for each day and for the days all together.

4. SYNOPTIC AND MESOSCALE ENVIRONMENT

Synoptic environment along the 27 events was mainly characterized at 500 hPa and 300 hPa by the presence of one of the next configurations:

- Deep transient Atlantic trough (clearly identified at 500 hPa or above) with or without a cold front associated, and diffluent flow.
- Westerly or south-westerly diffluent flow with embedded transient short wave, better identified in WV imagery.
- Centered cold low over Iberian Peninsula.

Only in one event a short wave ridge was present over the study area associated to a low centered 1000 km westward. Anyhow, flow through the ridge was diffluent again.

Although in satellite imagery and frontal charts well defined synoptic cold or occluded fronts are rare (only 6 cases) mesoscale surface boundaries and high levels fronts have been present most of the days.

The selection of a set of hailstorms episodes introduce, of course, a bias in the distribution of meteorological situations that have been present, characterized by notable synoptic forcing. This bias probably introduces a bias in the characteristics of the convection initiation and evolution that limits the generality of the results presented here. On the other hand, climatology shows that deep and/or organized convection it is very difficult to develop in the study area without a clear synoptic or mesoscale forcing.

5. CONVECTIVE SYSTEMS CHARACTERISTICS

The analyzed convective episodes have been classified as:

- One event with a wide area of stratiform precipitation and embedded convective cells.

- Nine events with one or more well defined squall lines with or without trailing stratiform area. Single isolated cells may be also present.

- Seventeen events with presence of isolated single cells or cell clusters.

The categories showed above have been obtained observing the complete radar domain.

A further analysis carried out to identify hypothetical convergence lines has shown a great tendency for cells to line up in more or less straight lines oriented frequently from southeast to northeast.

The more frequent convective structures displacements, resulting from the combination of propagation and translation components, have been from southwest to northeast and from west to east, with some anomalous displacements from the southeastern mountains (Fig. 3) to northwest. Apparent convective lines also moved frequently from southwest to northeast associated frequently to the pass of cold fronts or mesoscale boundaries.

6. RESULTS AND DISCUSSION

A set of 279 new 2D potentially convective structures (CEL0) have been identified inside the rectangular area (Fig. 3).

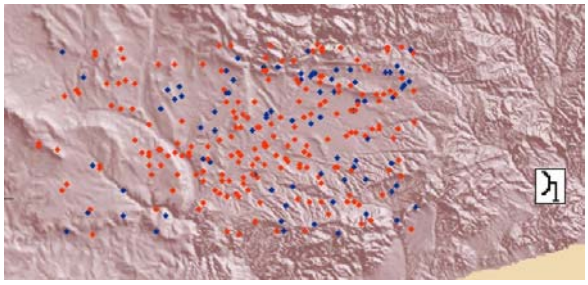

Fig. 3. Storm initiation locations over an orographic basis. Blue dots: artifacts. Red dots: Meteorological cells. Notice the mountains in the southeastern corner of the study area.

After YRADAR execution a subjective detailed analysis of convection initiation, development and evolution from radar imagery have been carried out. The first conclusion obtained is that it must be very careful when interpreting the plot of the supposedly new convective cells. Schematics as shown in Fig. 4 have been built to analyze convective events. These schematics can be simple or very complex depending on the duration of the episode, the triggering mechanisms, the number of new cells developed and the frequency and kind of interactions between them. For example, 26 real splits and 21 real mergings have been detected during the whole of the episodes.

The examination of the 27 PPI0 loops has shown a set of artifacts that have been considered new convective cells by the method applied. After the subjective filtering of the artifacts, 196 (70.3 %) cells have been considered meteorological new cells (CEL0M), 26 of them because of splitting, and 83 artifacts.

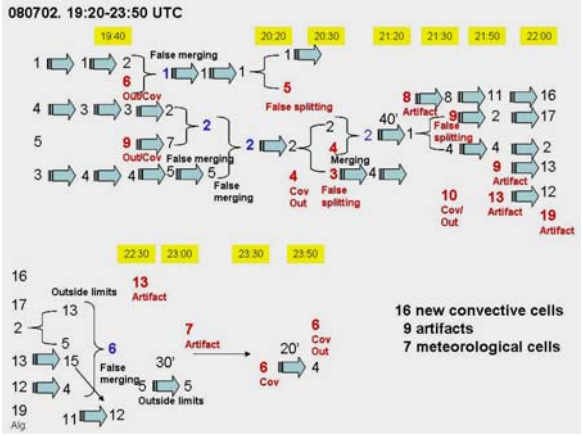

Fig. 4. Example showing the evolution of the automated identified and tracked potentially convective cells observed during the 8 July 2002, between 19:20 UTC and 23:50 UTC. Black numbers: Number of old convective cell. Red numbers: New cells. Yellow numbers: Initiation times. Merges and splits are also indicated. Cov: Triggering in convergence lines. Out: Gust front triggering.

The high proportion of artifacts (30 %) justify removing them from the database of new convective cells. The artifacts are mainly:

- 2D radar structures resulting from false splitting. False splitting may appear from breakage of a 2D structure as a consequence of orographic beam blockage or path attenuation, for example. In many cases, after a short time a merging rebuilds previous structure.

- Old cell rebirth. Sometimes, a 2D structure can lose the category of convective either as a consequence of internal real changes or because of observational difficulties. Anyhow, from the point of view of the identification of favorable areas to developing convection, rebirth cells (cells appeared again) would not be considered new cells. In Fig. 5 an example of cell rebirth is showed. Convective cell labeled 10 vanishes at 13:10 UTC appearing again 10 minutes later as the structure 5. At 13:10 UTC structure labeled 8 appears. Again, radar beam blockage or beam attenuation by rain could be responsible of these artifacts.

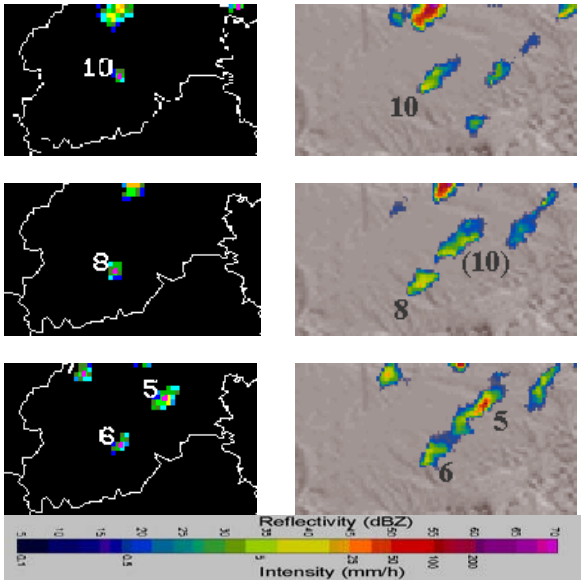

Fig. 5. Example of old cell rebirth in study area. 19 September 2000. Left: 13:00 UTC. Centre: 13:10 UTC. Right: 13:20 UTC. Top: Convective images obtained from YRADAR. Bottom: Reflectivity images. First PPI.

- Single cell-multicell alternation. 2D radar structures analysis frequently considers multicell storms as single cell storms with a unique centroid. Sometimes, during multicell storm motion and evolution "convective bridges" between local reflectivity maxima break producing lose of contiguity in reflectivity field. Then, one or more old convective cells are considered new cells.

- Ground clutter echoes intensification under anaprop conditions. Anaprop conditions may be present even during convective episodes. Ground echoes associated are very difficult to eliminate and therefore have been considered new convective cells.

- Incorrect tracking due to lack of wind data or extreme clustering. In this study wind data has not been used to assign 2D radar structures present in time *t* to structures present in time *t-10'*, and as a consequence, in a very few number of cases assignation has been incorrect (In operationally tasks YRADAR effectively uses wind data). Clustering also introduces uncertainty in tracking processes (Howard *et al.* 1997).

A quick look of the image loops shows a clear tendency to convective cells clustering that make difficult to track the cells and therefore establish them as new cells or not. This spatial distribution also suggests the presence of local or mesoscale triggering mechanisms, probably associated to stationary or transient planetary boundary layer convergence zones (Wilson and Schreiber 1986; Koch and Ray 1997).

Some methods have been tested to automatically identify artifacts. The first one consists in labeling CEL0 having a lifetime of 10 '(present in a single radar image). A 50 % of the artifacts (CEL0F) agree with this condition while only a 37 % of the meteorological cells CEL0M do it. This result shows a slightly more ephemeral nature of the artifacts.

The second method proposed consists in analyze the distribution of distances (D0) between the new convective cells in the rectangular area and all the cells scattered over the complete radar domain at time *t* and the distribution of distances (D1) between the new convective cells present at time *t* and all the cells present at time t-10'.

Location, orientation and dimensions of the rectangular area determine that maximum distance possible between two centroids is 430 km. In fact, maximum values obtained have been 379 km and 375 km for D0 and D1 respectively.

Table 2 shows the main statistical parameters extracted from the 2905 values for D0 and 2429 for D1. Each cell resulting from real (meteorological) splitting have also been identified and labeled with number 2.

ID	All classes	0	1	2	S	L
D0min	31	31	31	25	24	35
D1min	30	28	32	19	27	32

Table 2. Statistical parameters of the distributions of distances between centroids. ID: Cell class. D0min, D1min: Mean value of the D0 and D1 minimum distances respectively. 0: Artifacts. 1: Meteorological new cells. 2: Cells resulting from splitting. S: Lifetime =10'. L: Lifetime > 10'.

The nonparametric Mann-Whitney U-test has been used to verify if differences between statistical parameters for different cell classes are significant. The results are: D0min(class 2) and D1min(2) are significantly lesser than D0min(class 0, class 1) and D1min(0,1) respectively. D0min(S) and D1min(S) are significantly lesser than D0min(L) and D1min(L) respectively. D1min(0) is significantly lesser than D1min(1). Therefore, artifacts and very short lived cells (36 % of those are artifacts) have a tendency to develop very near of previous cells.

Clustering tendency has been also analyzed showing some interesting results (Fig. 6 and Fig. 7):

- A 90% of D0 and D1 are lesser than 215 km (the half of maximum possible distance).

- A 90% of D0min is lesser than 60 km, a 50% lesser than 30 km and a 25% lesser than 15 km.

- A 90% of D1min(0) is lesser than 40 km.

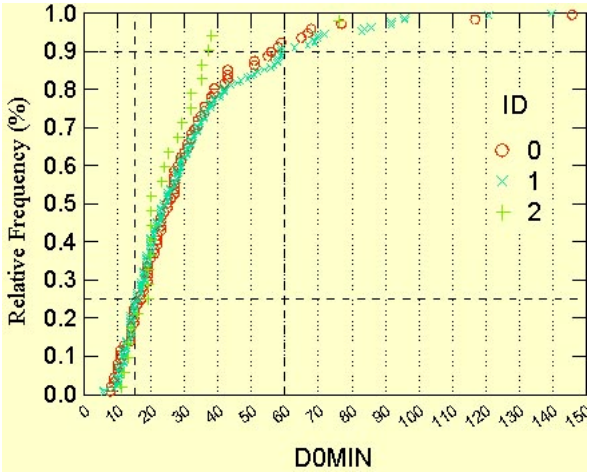

Fig. 6. Cumulative relative frequency of D0MIN for cells class 0, 1 and 2.

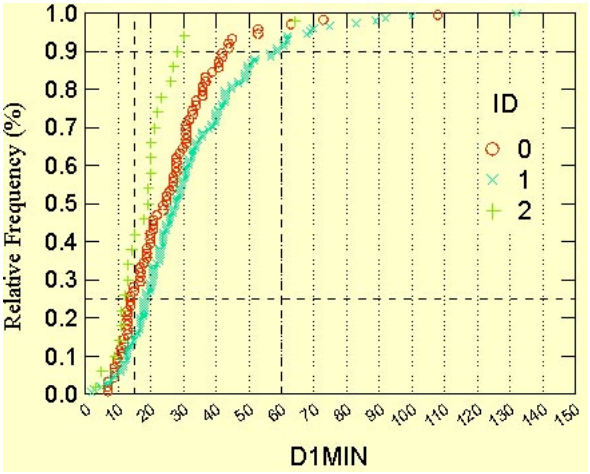

Fig. 7. Cumulative relative frequency of D1MIN for cells class 0, 1 and 2.

Therefore, it may be concluded that clustering responds to mesoscale environment and convective scale dynamics but it is also associated to the presence of the artifacts.

The plotting of the centroids over the rectangular (Fig. 8) area shows an apparently random distribution but it is important to notice that the spatial distribution of CEL0F shows a greater dispersion than that of CEL0M. Moreover, the center of CEL0F population is slightly displaced northeastward respect the center of CEL0M population. This displacement could be associated to the fact that most of the cell paths cross the northeastern corner of the area. Finally, using a nonparametric kernel density estimator it is possible to show that spatial density maximums of CEL0M and CEL0F are located at different places showing again that its location responds to different processes.

Daily distribution of the new cells number (NCEL0T) shows a great dispersion. Daily minimum and maximum are 0 and 28 respectively, mean is 10.7 and standard deviation 7.1.

The minimum value corresponds to an episode in which a unique convective storm crossed the area from northwest to southeast but any new convective cell developed.

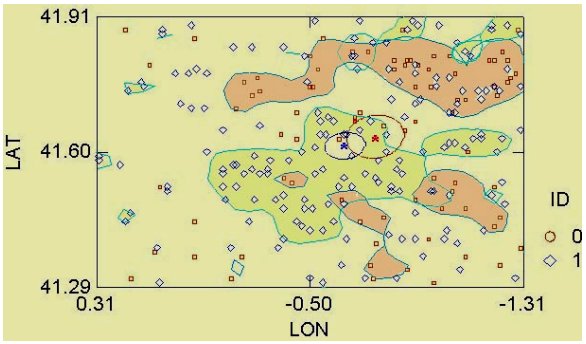

Fig. 8. Storm initiation locations for cells class 0 and 1. Blue asterisk and ellipse: centroid of meteorological cells population and confidence ellipse (p=0.95). Red asterisk and ellipse: centroid of artifacts population and confidence ellipse (p=0.95). Local maximums of concentrations have been showed applying a nonparametric kernel density estimator (p=0.150). Green and orange colored areas show these maximums.

Statistical parameters for filtered database (NCEL0M) are a maximum of 22, a mean value of 7.5 and a standard deviation of 5.3. This distribution shows less dispersion than previous one but still has a long tail from NCEL0M=15 to NCEL0M=22, associated to three episodes with an abnormal degree of convection generation (Fig. 9).

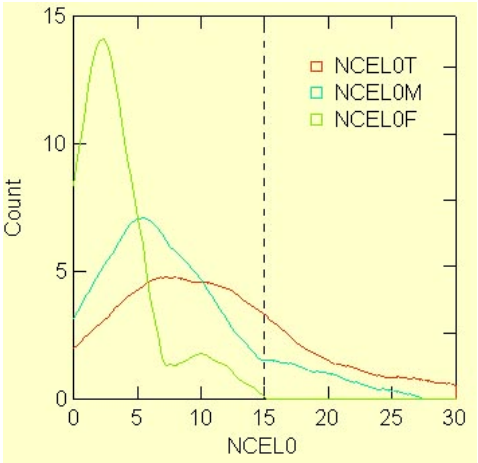

Fig. 9. Kernel density functions for NCEL0T, NCEL0M and NCELF. NCEL0= Number of new convective cells.

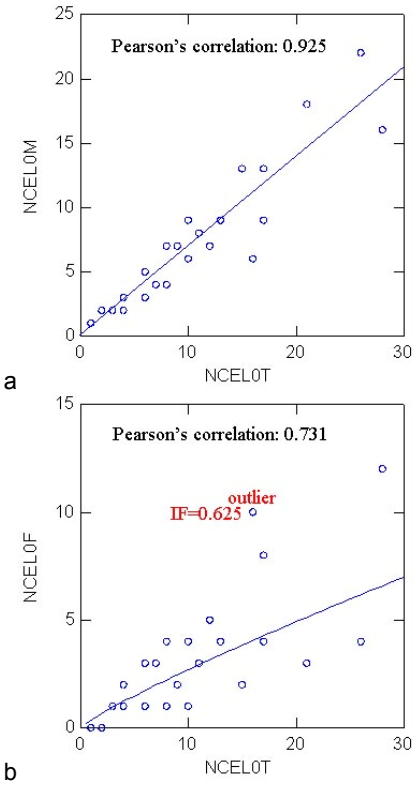

Fig. 10. Scatterplot of NCEL0T vs NCEL0M (a) and vs NCEL0F (b) and Pearso'n correlation coefficient. IF= NCEL0F/ NCEL0T.

These three episodes are included between the five longest episodes, defining duration as the lapse between the time of the first identification and the last one. In fact, Pearson correlation coefficient between NCEL0M and duration is 0.852, showing NCEL0M a quasi-lineal dependence with duration, better defined for durations greater than 4 hours.

Correlation between NCEL0T and the daily number of artifacts (NCEL0F) and between NCEL0F and duration are worse than values given before suggesting dependence with more complex factors that introduce non linearity: absolute location and motion of convective cells over the radar domain and relative between them (Fig. 10 and Fig. 11).

One of the factors that can have influence on NCEL0M is instability. Lifted (LI), Total Totals (TT) and K indices from Zaragoza 00 UTC and 12 UTC soundings have been correlated with NCEL0M obtaining very low values of correlation. Correlation has been also calculated between indices coming from the most recent sounding to the time of the first identification obtaining low values again. Afterwards, taking into account the great dependency between NCEL0M and the duration of the episode, a new coefficient of correlation has been calculated between the indices and NCEL0M normalized by dividing by duration showing still low values but somewhat better.

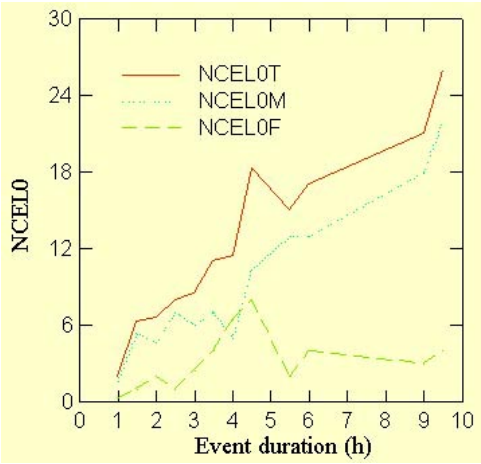

Fig. 11. Number of convective new cells vs event duration.

TT seems to be the better correlated index (Fig. 12). CAPE and precipitable water values have also been analyzed showing low correlations.

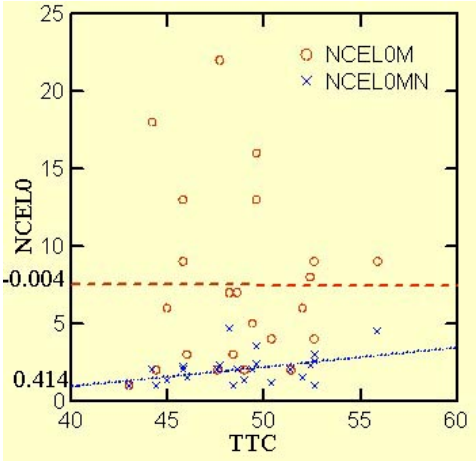

Fig. 12. Scatterplot of NCEL0 vs TTC. NCEL0MN: Normalized NCEL0M. TTC: Total totals index extracted from the most recent sounding to convective episode onset.

Therefore, from this analysis it is possible to suggest that convective activity defined as the number of cells developed during the episode depends primarily of other factors like the triggering mechanisms time-space characteristics and their effectiveness.

After filtering artifacts, an analysis of possible triggering mechanisms has been carried out. Splitting has been considered a process that generates new convective cells but not a triggering mechanism. New convective cells have been classified as first generation or second generation convection regarding if they are associated or not to previous cells.

Two mechanisms have been considered here as responsible of second generation convection: gust front triggering and discrete propagation (Houze 2004) although in this study any effort has been made to discriminate between them. Fig. 13 shows an example of convection initiation ahead a well defined eastward moving squall line. Convective cell labeled 4 at 17:20 UTC probably develops in the interaction between a gust front or a gravity wave associated to the linear mesoscale convective system and some kind of stationary convergence line apparent from small convective cells alignment. Cell 4 (after labeled 5) remains stationary over one of these lines and eventually merges with squall line (multicell storm 1).

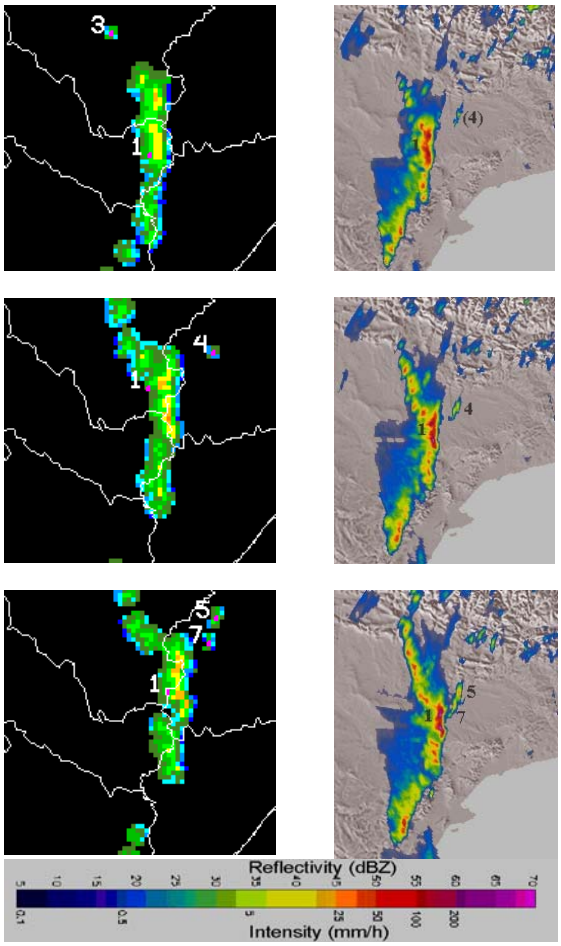

Fig. 13. Example of cell development a few kilometers ahead a squall line. 4 June 2002. Top: 17:10 UTC. Center: 17:20 UTC. Bottom: 17:30 UTC. Left: Convective images obtained from YRADAR. Right: Reflectivity images. First PPI.

First generation convection is supposed to be always linked to some kind of planetary boundary layer convergence zone.

Orography seems have not play a very relevant role in determining the new convective cells location except for the southeastern corner of the rectangular area, where mountainous terrain is present (Fig. 5).

Although it is very difficult to specify the exact mechanisms that trigger convection, the detailed analysis of location and motion relative between new and previous cells and the dimensions and evolution of convective structures has suggested that in these episodes downburst-producing storms or convective gravity waves (discrete propagation) have reported for at least 20% of meteorological cells class 1.

Another detailed subjective radar imagery dynamical analysis has been made over the whole domain to identify the hypothetical convergence lines that could have affected study area. As in Pascual and Callado 2002, this analysis has been carried out in “precipitating” air, i.e., when precipitation is already detectable. In some cases, satellite imagery has been used to support radar analysis. To define these convergence/convective lines the next hypotheses have been applied:

- 2D convective radar structures alignment must be supported by a convergence line.
- Convective cells spatial distribution and relative motion between them have to be coherent with physical definition of convergence line.
- Convergence lines location, orientation and motion (both absolute and relative between them) have to maintain an internal coherence and coherence with synoptic and mesoscale environment during the event.

Taking into account these constraints, 100 convergence/convective lines have been identified. Gust fronts are not included in this set of convergence lines.

Their characteristics are

- Daily distribution: Maximum: 9. Minimum: 0 (3 days).
- Main orientation: SW-NE. This orientation is coherent with most frequent synoptic and mesoscale boundaries orientations (Fig. 14).
- Main directions of motion: W to E and SW to NE. This motion is coherent with the most frequent through and synoptic fronts motion.
- Degree of mobility: 80 % moving; 20 % stationary. Both types of lines have been simultaneously present in some events indicating their different origins. Stationary lines are most of cases orographically induced lines while moving lines are linked to transient disturbances.

- Most frequent lengths: Between 60 km and 200 km. Convective/convergence lines affecting rectangular area generally extend outside their limits.

- Most frequent duration: 2-3 hours.

This analysis also has shown that new convective cells develop mostly along these lines.

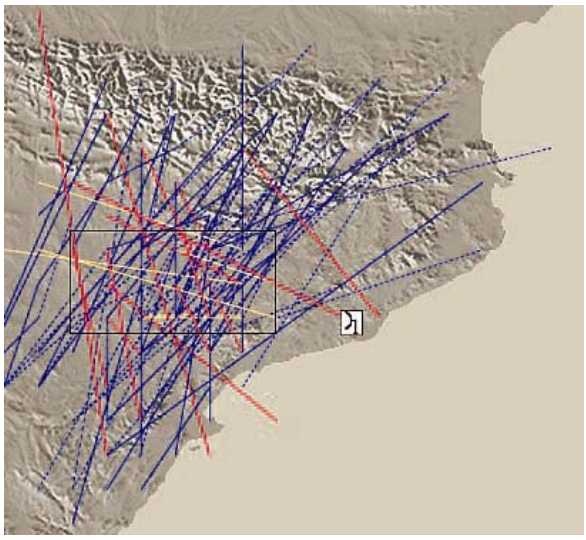

Fig. 14. Synthetic convective/convergence straight lines occurring during the selected 27 episodes. Different line colors and styles are used only for clarity.

Finally, the interpretation of daily plots of new convective cells locations (static analysis) in terms of convergence lines has been considered. This task has lead to conclude that appearance of new convergence lines, their motion, interactions and extinction distribute centroids locations without any linear orientation. The high ratio of secondary cells also distorts potentially linear distributions adding centroids some kilometers ahead of convergence lines.

7. CONCLUSIONS

To obtain some radar-based general results about timing and location of convection initiation in a determined area it is necessary to hand enormous quantity of information and as a consequence is desirable to have some automated objective methods capable to carry out a correct identification and tracking of convective cells. Nevertheless, inherent features associated to observational method and algorithms characteristics, normally defined to analyze intense convection and/or mature cells, restrict the validity of the results obtained.

This paper has tried to identify for 27 hail events in western Catalonia the artifacts that have appeared after the execution of the objective methods and characterize them with the aim to suggest a filtering automated method.

2D radar structures resulting from false splitting, old cell rebirth, single cell-multicell alternation, ground clutter echoes intensification under anaprop conditions and incorrect tracking due to lack of wind data or extreme clustering are the main factors that have created artifacts.

The distances distribution between new convective and old cells both calculated at the same time and between two images separates ten minutes shows that artifacts have a great tendency to be significantly closer to old cells than meteorological cells. In addition, lifetime distribution shows that artifacts have a more slightly ephemeral nature. Some automated process that uses these artifacts qualities could be applied to filter a high number of them although some meteorological would be also removed.

Spatial distribution of artifacts shows a greater dispersion than that of meteorological new cells and gravity centre of its population is displaced slightly northeastward respect the meteorological gravity centre, showing the dependence with the storm paths identified and may be with the relative minimum of beam blockage north of the band of maximum blockage.

The poor correlation between the number of artifacts and the duration of the events suggests dependence with more complex factors that introduce non-linearity: absolute location and motion of convective cells over the radar domain and relative between them.

After filtering artifacts, it is possible to extract some conclusions about convection initiation during the set of 27 days selected.

Convective activity depends primarily of factors like the triggering mechanisms time-space characteristics and their effectiveness.

Secondary convection has an important role in generating new convection due probably to the flat character of the study area and to the notable number of great convective structures and mesoscale convective systems.

Visual analysis of convective cells time-space distribution and motion has lead to conclude that they appear mostly organized in more or less straight lines which dimensions and evolution have been coherent with synoptic and mesoscale environment. These lines have been considered convergence lines in

order to account of the high proportion of new meteorological convective cells appeared over there.

Acknowledgements

Thanks are due to the Spanish Instituto Nacional de Meteorología for providing data and support.

We would like to particularly thank Alfons Callado (INM-Barcelona) and Marc Berenguer (GRAHI UPC-Catalonia) for their many contributions. Also thanks to Fermin Elizaga and Francisco Martin (INM-Madrid) for their very interesting suggestions and discussions.

8. References

Carretero Porris, O., 2001: Procedimiento de identificación, seguimiento y extrapolación de células en 3 dimensiones. V Simposio de Predicción del Instituto Nacional de Meteorología. Madrid (Spain), 20-23 November 2001.

Houze**,** R. A., Jr., 2004: Mesoscale convective systems. *Rev. Geophys.*, **42**, 0.1029/2004RG000150, 43 pp.

Howard, K. W., J. J. Gourley and R. A. Maddox, 1997: Uncertainties in WSR-88D measurements and their impacts on monitoring life cycles. *Weather and Forecasting*, **12**, 166-174.

Koch, S. E. and C. A. Ray, 1997: Mesoanalysis of summertime convergence zones in central and eastern North Carolina. *Weather and Forecasting*, **12**, 56-77.

Martín, F. 2001. Identificación objetiva de estructuras convectivas a partir de los datos radar del PPI/CAPPI bajo en MCIDAS. V Simposio Nacional de Predicción. Instituto Nacional de Meteorologia. Madrid (Spain), 20-23 November 2001.

Pascual, R. and A. Callado: 2002. Mesoanalysis of recurrent convergence zones in north-eastern Iberian Peninsula. Preprints, *2nd European Conference on Radar Meteorology*, Delft, The Netherdlands, ERAD, 59-64.

Pascual, R., A. Callado and M. Berenguer, 2004: Convective storm initiation in central Catalonia. Third European Conference on Radar Meteorology (ERAD) in conjunction with COST 717 Final Seminar. Visby (Sweden), 6-10 September 2004.

Rasmussen, C. and G. D. Hager, 2001: Probabilistic data association methods for tracking complex visual objects. *IEEE transactions on pattern analysis and machine intelligence*, **23**, 560-576.

Sempere-Torres, D.; Sanchez-Diezma, R.; Berenguer, M.; Pascual, R.; Zawadzki, I. 2003. Improving radar rainfall measurement stability using mountain returns in real time. 31th Conference on Radar Meteorology. Seattle (USA), 6-12 August 2003.

Steiner, M.; Houze, R. A.; Yuter, S. E. 1995. Climatological characterization of three dimensional storm structure from operational radar and raingauge data. Journal of Applied Meteorology, **34**, 1978-2007.

Wilson, J.W. and W. E. Schreiber, 1986: Initiation of convective storms at radar-observed boundary-layer convergence lines. *Monthly Weather Review,* **114,** 2516-2536.